Coherent two-dimensional terahertz-terahertz-Raman spectroscopy

Ian A. Finneran[a], Ralph Welsch[a], Marco A. Allodi[a,1], Thomas F. Miller III[a], and Geoffrey A. Blake[a,b,2]

[a]Division of Chemistry and Chemical Engineering, California Institute of Technology, Pasadena, CA 91125; and [b]Division of Geological and Planetary Sciences, California Institute of Technology, Pasadena, CA 91125

Edited by Michael L. Klein, Temple University, Philadelphia, PA, and approved May 6, 2016 (received for review April 7, 2016)

We present 2D terahertz-terahertz-Raman (2D TTR) spectroscopy, the first technique, to our knowledge, to interrogate a liquid with multiple pulses of terahertz (THz) light. This hybrid approach isolates nonlinear signatures in isotropic media, and is sensitive to the coupling and anharmonicity of thermally activated THz modes that play a central role in liquid-phase chemistry. Specifically, by varying the timing between two intense THz pulses, we control the orientational alignment of molecules in a liquid, and nonlinearly excite vibrational coherences. A comparison of experimental and simulated 2D TTR spectra of bromoform ($CHBr_3$), carbon tetrachloride (CCl_4), and dibromodichloromethane (CBr_2Cl_2) shows previously unobserved off-diagonal anharmonic coupling between thermally populated vibrational modes.

ultrafast dynamics | terahertz | coherent multidimensional spectroscopy

Detailed molecular pictures of the structure and dynamics of liquids drive our understanding of chemistry and biology. Nonlinear 2D infrared and NMR spectroscopies have revealed many specifics of liquid behavior, monitoring the coupling, spectral diffusion, and homogeneous linewidths of intramolecular vibrations and nuclear spins (1, 2). However, the motions that directly participate in solvation and chemical reactivity are manifest in the terahertz (THz) region of the spectrum, making 2D THz studies especially valuable. To date, no 2D technique has been demonstrated that incorporates multiple THz interactions with a liquid.

Recent advances in pulsed, high-power THz sources with electric fields exceeding 100 kV/cm have enabled a new generation of nonlinear THz spectroscopy, in which THz radiation is used to both manipulate and record the response of matter (3). It is now possible, for example, to control the alignment of gas-phase molecules (4) and antiferromagnetic spin waves (5), drive an insulator-to-metal transition in oxides such as VO_2 (6), and break up Cooper pairs in a superconductor with intense THz pulses (7). Nonlinear THz interactions have also enabled the first demonstrations of 2D THz spectroscopy in a double quantum well system and graphene (8, 9).

With weak transition dipole moments yet high THz absorptivity, liquids present many challenges with respect to the development of 2D THz spectroscopy. Initial successes with 2D Raman spectroscopy were later shown to suffer from the interference of cascaded processes (10–12), but new schemes using optical pulse shaping have eliminated the cascaded contributions (13). An alternative approach is resonant 2D THz spectroscopy, analogous to 2D IR spectroscopy. However, this method is hindered by a lack of THz directional phase matching, leading to signals that can be easily overwhelmed by a strong linear background. In the last few years, hybrid optical-THz techniques that circumvent these challenges have emerged, including 2D Raman-THz spectroscopy and THz Kerr effect spectroscopy (14–16). Here, we present the complementary 2D TTR spectroscopy, a natural extension of these hybrid techniques, that was described theoretically by Cho in 1999 (10, 17, 18). To our knowledge, 2D TTR is the first 2D experimental technique applicable to liquids that is nonlinear in the THz field, and it is sensitive to the anharmonicity of molecular vibrations and the molecular orientational alignment. In these first experiments, the power of this technique to explore molecular dynamics and interactions is demonstrated in simple halogenated liquids. With modest improvements in sensitivity, 2D TTR should be suitable for studies of intermolecular and intramolecular vibrational heterogeneity in biological macromolecules, amorphous solids, and hydrogen-bonded liquids.

Results and Discussion

The 2D TTR experiment (Fig. 1*A*) uses two intense carrier-envelope-phase (CEP) stable THz pump pulses followed by a weak 40-fs near-infrared (NIR) probe pulse. By adjusting the delay t_1 between THz pulses, we control the phase of the THz radiation at the sample while maintaining a constant power. The heterodyne-detected transient birefringence is measured along the t_2 axis with the NIR probe pulse from the same laser system. By Fourier transforming over the t_1 and t_2 times, one can generate 2D plots in the frequency domain. In an isotropic medium, such as a liquid, the lowest-order contribution to the measured nonlinear polarization is given by (15, 19)

$$P^{(3)}(t) = \iint dt_1 dt_2\, R^{(3)}(t_1, t_2) E_B(t - t_2) E_A(t - t_1 - t_2) E_{nir}(t), \quad [1]$$

where $R^{(3)}(t_1, t_2)$ is the third-order response function of the liquid, $E_A(t - t_1 - t_2)$ and $E_B(t - t_2)$ are the two THz pulses, and $E_{nir}(t)$ is the NIR probe pulse. Weaker single-pulse third-order responses are removed by differential chopping (*SI Appendix*, *Experimental Setup*).

Significance

The thermally populated motions of liquids, including hydrogen bonds, low-energy bending vibrations, conformational torsions, and hindered rotations, are resonant in the terahertz region of the spectrum. These motions regulate solvation, macromolecular structure, and vibrational energy flow in liquid-phase chemistry. By exciting terahertz motions nonlinearly with multiple pulses of terahertz light, we can measure their anharmonic coupling and distribution of chemical environments. We can also begin to control their quantum coherence and population, a critical step forward in the control of liquid-phase chemistry with light.

Author contributions: I.A.F., M.A.A., and G.A.B. designed research; I.A.F. and R.W. performed research; I.A.F., R.W., M.A.A., T.F.M., and G.A.B. analyzed data; and I.A.F., R.W., M.A.A., T.F.M., and G.A.B. wrote the paper.

The authors declare no conflict of interest.

This article is a PNAS Direct Submission.

[1]Present address: Department of Chemistry, the Institute for Biophysical Dynamics, and the James Franck Institute, The University of Chicago, Chicago, IL 60637.

[2]To whom correspondence should be addressed. Email: gab@gps.caltech.edu.

This article contains supporting information online at www.pnas.org/lookup/suppl/doi:10.1073/pnas.1605631113/-/DCSupplemental.

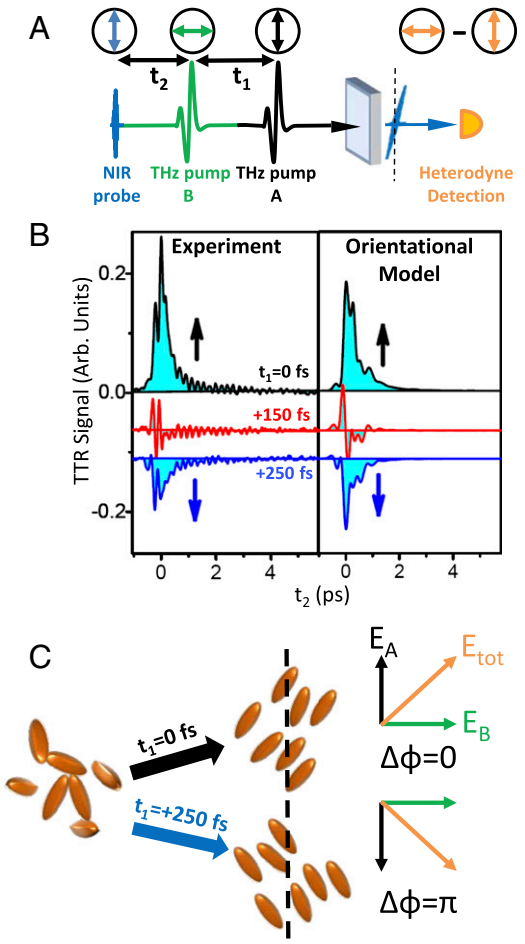

Fig. 1. An overview of the 2D TTR experiment. (*A*) The pulse sequence used in this work includes two intense THz pulses separated by time delay t_1, followed by a weak NIR probe pulse at delay t_2. The signal is measured as a birefringence of the NIR probe pulse and is sensitive to changes in molecular polarizability. The polarizations of the light fields are shown in the circles above the pulses. (*B*) By controlling the phase overlap of two high-field THz pulses in liquid $CHBr_3$, a positive ($t_1 = 0$ fs) or negative ($t_1 = 250$ fs) signal corresponding to the birefringence can be generated. Multiexponential contributions from intermolecular vibrations and librations are present near $t_2 = 1$ ps. At other times ($t_1 = 150$), the orientational birefringence is dampened. (*C*) The proposed molecular mechanism causing a sign change in the birefringence is due to control of the electronic polarizibility and orientational alignment of the molecules in the sample.

We illustrate the principal components of a 2D TTR response function with the birefringent signal from liquid bromoform at 295 K (Figs. 1*B*, *Left* and 2*A*). For the $t_1 = 0$ fs trace (Fig. 1*B*, *Left*, black line), the electronic response is visible as a sharp peak near $t_2 = 0$ ps, which follows the E-field^2 (including phase) of the THz radiation (15). An exponential decay extending to $t_2 = 2$ ps results from the rotational diffusion of the molecules in the liquid as they reorient after aligning with the THz field (15). Nonlinear vibrational coherences from the excitation of the $\nu 6$ mode are visible as a damped oscillation out to $t_2 = 4$ ps (16). As t_1 is shifted to 150 fs (red line), the transient birefringence is attenuated, whereas, at 250 fs (blue line), the response becomes negative. A full 2D scan of this t_1-dependent control is shown in Fig. 2*A*.

To understand the observed birefringence control, we return to the 2D TTR pulse sequence (Fig. 1*A*). The polarizations of the THz pump pulses are orthogonal (shown in the black circles), and CEP is stable. By changing the phase offset ($\Delta\phi$) between the pulses, or t_1, we change the polarization of the total THz field (E_{tot}) when the pulses are overlapped in time (Fig. 1*C*). At $t_1 = 0$ fs, $\Delta\phi = 0$, and E_{tot} is oriented at +45 degrees with respect to the probe, whereas, at $t_1 = 250$ fs, $\Delta\phi = \pi$, and E_{tot} is oriented at +135 degrees with respect to the probe.

The electronic and nuclear alignment of the molecules follows the polarization of the THz radiation (15, 16). Thus, we posit that the change in the measured birefringence as a function of t_1 is due to angular control of the molecular alignment induced by the THz polarization (Fig. 1*C*). A simple orientational model of this behavior using the measured THz electric fields is shown in Fig. 1*B*, *Right*; it is an extension of the model used in our previous work (ref. 16 and *SI Appendix*, *Orientational Model*). The orientational model correctly predicts the sign changes and zero crossings of the birefringence, although it does not account for the nonlinear vibrational coherences. Thus, by varying the phase of the THz polarization at the sample, one can control the orientation of molecules in a liquid.

We now consider the damped oscillation shown in Figs. 1*B*, *Left* and 2*A*. This component is due to the excitation of intramolecular vibrational coherences, and it provides information on the coupling and anharmonicity of vibrations in the liquid. It is best visualized with a 2D Fourier transform along the t_1 and t_2 axes starting at $t_2 = 1$ ps, after detrending the orientational response with a single exponential fit for each t_2 scan (Fig. 2*B*).

The origins of the 2D TTR signatures can be derived using third-order perturbation theory on a three-level system, yielding 24 rephasing and nonrephasing Liouville pathways (*SI Appendix*, *Perturbative Density Matrix Derivation*). With phase-sensitive heterodyne detection, rephasing and nonrephasing Liouville pathways are differentiated in a 2D Fourier transform. Signals in the first quadrant ($f_1 = \pm$, $f_2 = \pm$) are nonrephasing, whereas signals in the second quadrant ($f_1 = \pm$, $f_2 = \mp$) arise from rephasing pathways (8, 19). The bandwidth (0.5–4 THz) of the THz pulses restricts the experiment to eight of the 24 pathways, all nonrephasing, two of which

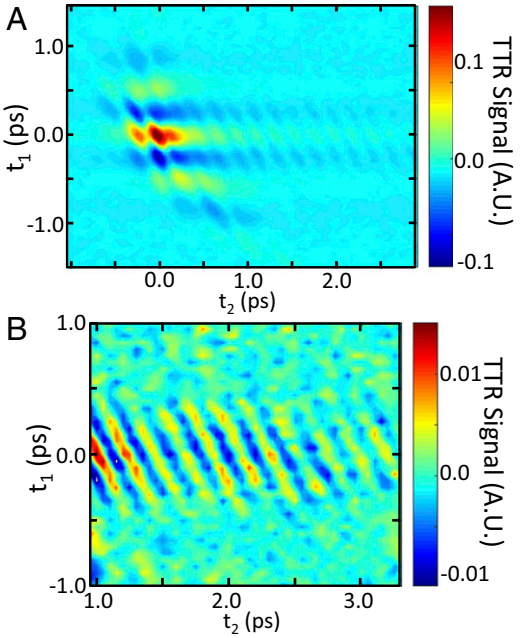

Fig. 2. Representative time domain 2D TTR signals. (*A*) The 2D time domain response of liquid bromoform. (*B*) Cutting the response in *A* beyond $t_2 = 1$ ps and detrending fits isolates the vibrational coherences.

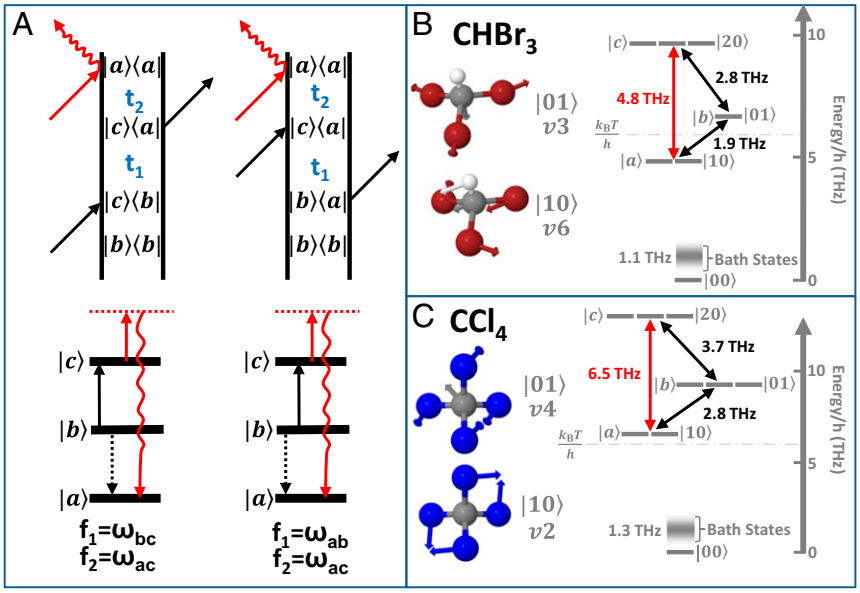

Fig. 3. A quantum mechanical description of the measured signals. (*A*) Two of 24 Liouville pathways in the 2D TTR experiment for generalized eigenstates $|a\rangle$, $|b\rangle$, and $|c\rangle$. (*B* and *C*) The energy levels and observed couplings in (*B*) $CHBr_3$ and (*C*) CCl_4. THz excitations are shown in black, Raman in red.

are shown in Fig. 3*A*. The sum of the eight pathways yields a response function $R^{(3)}(t_1, t_2)$ given by

$$R^{(3)}(t_1, t_2) \propto \mu_{ab}\mu_{bc}\Pi_{ac}\left(p_{ab}e^{-i\omega_{ab}t_1}e^{-i\omega_{ac}t_2} - p_{bc}e^{-i\omega_{bc}t_1}e^{-i\omega_{ac}t_2}\right) + c.c. \quad [2]$$

Here dipole and polarizability couplings are labeled as μ_{xy} and Π_{xy}, and the equilibrium population differences between states y and x as p_{xy} for the generalized three-level system. Thus, each peak in a 2D THz-THz-Raman spectrum results from a closed loop between three molecular eigenstates, hereafter denoted $|a\rangle$, $|b\rangle$, and $|c\rangle$. Coherences are initiated by THz pump A and seen on the t_1 time or f_1 frequency axis. THz pump B moves these coherences to a new eigenstate, analogous to a coherence transfer pulse in 2D NMR. The loop is closed with a $|c\rangle \rightarrow |a\rangle$ or $|a\rangle \rightarrow |c\rangle$ Raman transition on the t_2 time, or f_2 frequency, axis. Similar to 2D Raman and 2D Raman-THz spectroscopy, every closed loop contains one or more transitions forbidden in the harmonic approximation, allowing us to directly measure the molecular anharmonicity (11, 20).

In Fig. 4, we demonstrate the capabilities of 2D TTR in measuring vibrational anharmonicities with the spectra of bromoform ($CHBr_3$, 295 K), carbon tetrachloride (CCl_4, 295 K), and dibromodichloromethane (CBr_2Cl_2, 313 K). For all three liquids, we observe peaks on the f_2 Raman axis that match the known lowest-energy intramolecular vibrations: $\nu6$ in $CHBr_3$ [*SI Appendix*, *Reduced Density Matrix (RDM) Simulation*] $\nu2$ in CCl_4 (21, 22); and $\nu4$ and $\nu5$ for CBr_2Cl_2 (23). Returning to the closed-loop picture, the $|c\rangle \leftrightarrow |a\rangle$ Raman transition is clearly assigned to changes of one quantum in each of these low-energy modes. The remaining mystery is the identity of the intermediate state $|b\rangle$ in the closed loop, which can be determined by examining the f_1 positions of the peaks.

At ~ 300 K (k_BT/h = 6.2 THz), there is significant population in the low-energy vibrational and bath states of these liquids. Using linear Raman and THz spectra and Eq. **2**, we can predict the precise peak positions for coupling to different $|b\rangle$ states. For $CHBr_3$, we observe a doublet f_1 peak that is consistent with anharmonic coupling between $\nu6$ and $\nu3$, but not with anharmonic coupling of $\nu6$ to bath modes (Figs. 3*B* and 4*A*). CCl_4 exhibits a similar doublet on the f_1 axis that matches a $\nu2$–$\nu4$ coupling (Figs. 3*C* and 4*B*). Simulated spectra from a reduced density matrix (RDM) method [*SI Appendix*, *Reduced Density Matrix (RDM) Simulation*] show good agreement with the experimental results (Fig. 4 *A* and *B*, *Right*).

The thermally populated vibrational manifolds of CBr_2Cl_2 (Fig. 5) are more complicated than those of CCl_4 and $CHBr_3$, which leads to further possibilities for vibrational coupling. However, a simple RDM simulation with eigenstates from the linear Raman spectrum and weak anharmonic $\nu4 \leftrightarrow \nu7$ and $\nu5 \leftrightarrow \nu7$ coupling reproduces all of the observed peaks (Fig. 4*C* and *SI Appendix*, *Analysis of Experimental and RDM Simulated Spectra*), and gives us insight into the relative coupling strengths in this liquid. Specifically, we see that the two lowest-energy vibrational modes are more strongly coupled to $\nu7$ than to $\nu3$ and $\nu9$.

Summary

In summary, we have demonstrated, to our knowledge, the first 2D spectroscopy of liquids that is nonlinear in the THz field. With two time-delayed THz pulses and an NIR probe pulse, we can control the orientational alignment of molecules in a liquid and generate 2D THz-THz-Raman spectra that are sensitive to anharmonic vibrational coupling. We measure significant coupling in the lowest-frequency intramolecular modes of liquid $CHBr_3$, CCl_4, and CBr_2Cl_2.

The off-diagonal peaks measured in the 2D TTR spectra provide information that is not present in a 1D linear spectrum. Specifically, the linear THz peaks of a liquid reveal the energies of its molecular eigenstates, whereas the off-diagonal 2D TTR peaks show the coupling between these eigenstates. The features measured here are, by definition, cross peaks, because they correlate a frequency on the pump axis to a different frequency on the probe axis. This allows us, for example, to show that, in CBr_2Cl_2, $\nu4$ and $\nu5$ are most strongly coupled to $\nu7$—information unobtainable in a linear spectrum. These off-diagonal peaks also allow us to determine individual components of an inhomogeneously broadened feature in the linear spectrum. This is the case in $CHBr_3$ and CCl_4, which show an inhomogeneously broadened absorption from 0.1 THz to 3.5 THz (*SI Appendix*, *Reduced Density Matrix (RDM) Simulation* and refs. 21 and 22). It is impossible to resolve the components of these features with a linear measurement, as the broadening is intrinsic to the liquids. The 2D TTR spectra, however, reveal several distinct components due to difference band transitions between intramolecular modes.

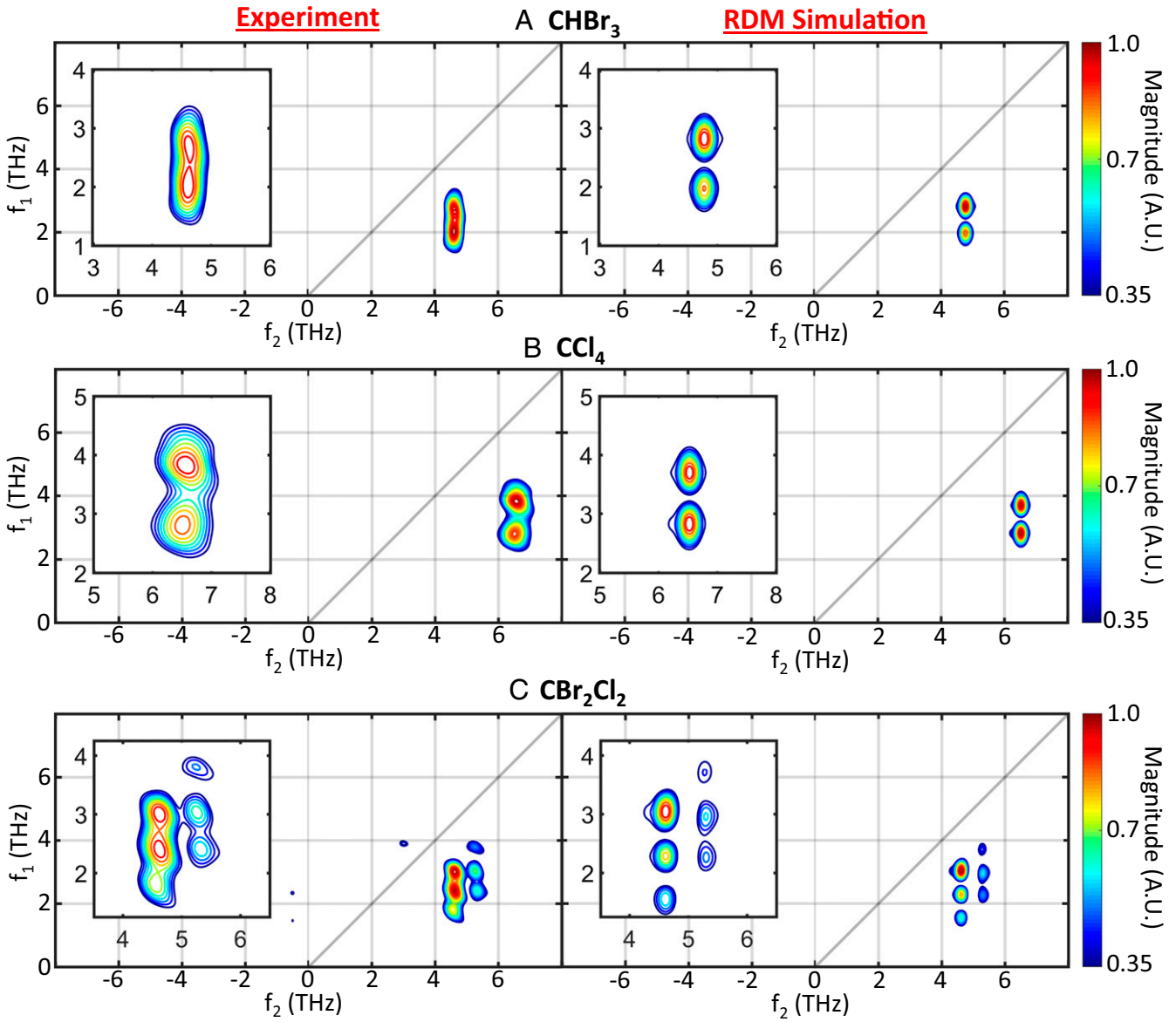

Fig. 4. Experimental (*Left*) and RDM simulated (*Right*) 2D TTR spectra of (*A*) $CHBr_3$, (*B*) CCl_4, and (*C*) CBr_2Cl_2. The f_1 axis corresponds to the THz pump, and the f_2 axis corresponds to the optical Raman probe.

Although limited in these first experiments, we expect 2D TTR sensitivity improvements of >100× using existing technologies (24, 25). Such improvements should enable the measurement of photon echo (rephasing) signals and permit studies of intermolecular vibrations in isotropic molecular solids and hydrogen-bonded liquids. The importance of THz-active motions in biochemistry is well documented (26), and 2D TTR studies could ultimately provide new insights on processes such as protein folding and DNA internal conversion.

Materials and Methods

Experiment. We generate 3.6-mJ pulses of 38 fs duration from an 800-nm Coherent Legend Elite USP Ti:Sa regenerative amplifier. The pulses from the amplifier are sent into an optical parametric amplifier (Light Conversion Ltd.) and downconverted to 1,450 nm (signal, 500 μJ) and 1,780 nm (idler, 330 μJ). The signal is routed through a delay line (t_1) and used to drive a 3-mm aperture 4-*N*,*N*-dimethylamino-4′-N′-methyl-stilbazolium 2,4,6-trimethylbenzenesulfonate (DSTMS) THz generation crystal (Rainbow Photonics). The idler is sent to a second DSTMS crystal. The two THz pulses are combined on a knife edge mirror, magnified by 7.5×, and focused on the sample with a 2-inch EFL 90-degree off-axis parabolic mirror. The peak field strengths of both pulses are ∼ 300 kV/cm. Liquids are held in a 1-mm-path-length Suprasil quartz cuvette. The transient birefringence in the sample is probed with a small portion of the 800-nm light from the amplifier, and sent down a second delay line (t_2). As described in our previous work, we heterodyne detect the transient birefringence using a 10^5:1 polarizer, a λ/4 plate, a Wollaston prism, and a pair of silicon photodiodes (16). The signal is isolated with differential chopping of the signal and idler beams and detected with a lock-in amplifier (*SI Appendix, Experimental Setup*).

Orientational Model. The electronic and orientational components of the measured signal are due to a change in the sample birefringence, or a difference in refractive index along the vertical and horizontal directions. The birefringent signal is predicted using the measured THz fields (15, 16). More details of the model are given in *SI Appendix, Orientational Model*.

RDM Simulation. An RDM approach (19, 27) is used to qualitatively simulate the 2D TTR spectra. The time evolution of the RDM ρ is given by the Liouville–Von Neumann equation

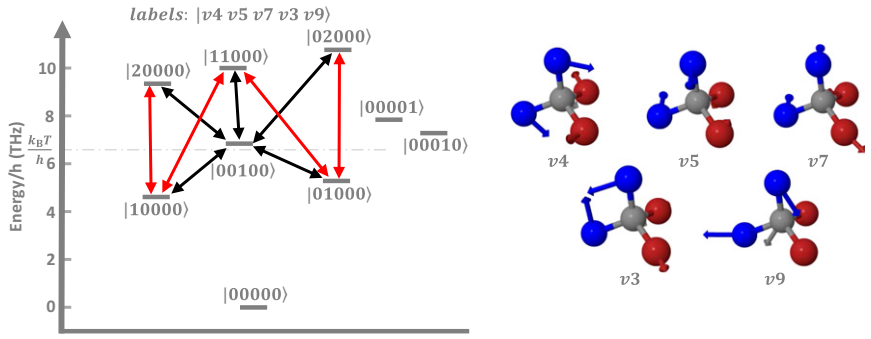

Fig. 5. The vibrational energy levels of CBr_2Cl_2. Observed THz excitations are shown as black arrows, and those for Raman excitations are in red.

$$i\hbar\frac{\partial\rho}{\partial t}=[\boldsymbol{H},\rho], \quad [3]$$

where $\boldsymbol{H}$ is the matrix representation of the Hamilton operator of the system under consideration. In this work, the time evolution is numerically calculated using a second-order differencing technique (28),

$$\rho(t+\Delta t)=\rho(t)-\frac{i}{\hbar}[\boldsymbol{H}(t),\rho(t)]2\Delta t-2\Gamma\Delta t, \quad [4]$$

where $\Gamma_{i,j}=(1-\delta_{i,j})(1/\tau_{i,j})$ defines the off-diagonal decay that is needed to phenomenologically incorporate dephasing caused by the surrounding bath, with an associated timescale $\tau_{i,j}$ (19, 27). A full list of parameters for the simulations is given in *SI Appendix, Reduced Density Matrix (RDM) Simulation*, and a symmetry analysis of the mode coupling is given in *SI Appendix, Symmetry Analysis*.

ACKNOWLEDGMENTS. The authors acknowledge the National Science Foundation (Grants CHE-1214123 and CHE-1057112 and the Graduate Research Fellowship Program) for financial support. R.W. acknowledges financial support from the Deutsche Forschungsgemeinschaft under Grant WE 5762/1-1. M.A.A. acknowledges current support from a Yen Postdoctoral Fellowship from the Institute for Biophysical Dynamics at the University of Chicago.

1. Ramasesha K, De Marco L, Mandal A, Tokmakoff A (2013) Water vibrations have strongly mixed intra- and intermolecular character. *Nat Chem* 5(11):935–940.
2. Macura S, Ernst R (1980) Elucidation of cross relaxation in liquids by two-dimensional NMR spectroscopy. *Mol Phys* 41(1):95–117.
3. Kampfrath T, Tanaka K, Nelson KA (2013) Resonant and nonresonant control over matter and light by intense terahertz transients. *Nat Photonics* 7(9):680–690.
4. Fleischer S, Field RW, Nelson KA (2012) Commensurate two-quantum coherences induced by time-delayed THz fields. *Phys Rev Lett* 109(12):123603.
5. Kampfrath T, et al. (2011) Coherent terahertz control of antiferromagnetic spin waves. *Nat Photonics* 5(1):31–34.
6. Liu M, et al. (2012) Terahertz-field-induced insulator-to-metal transition in vanadium dioxide metamaterial. *Nature* 487(7407):345–348.
7. Matsunaga R, Shimano R (2012) Nonequilibrium BCS state dynamics induced by intense terahertz pulses in a superconducting NbN film. *Phys Rev Lett* 109(18):187002.
8. Woerner M, Kuehn W, Bowlan P, Reimann K, Elsaesser T (2013) Ultrafast two-dimensional terahertz spectroscopy of elementary excitations in solids. *New J Phys* 15(2):025039.
9. Kuehn W, Reimann K, Woerner M, Elsaesser T (2009) Phase-resolved two-dimensional spectroscopy based on collinear *n*-wave mixing in the ultrafast time domain. *J Chem Phys* 130(16):164503.
10. Tanimura Y, Mukamel S (1993) Two-dimensional femtosecond vibrational spectroscopy of liquids. *J Chem Phys* 99(12):9496–9511.
11. Tokmakoff A, et al. (1997) Two-dimensional Raman spectroscopy of vibrational interactions in liquids. *Phys Rev Lett* 79(14):2702–2705.
12. Wilson KC, Lyons B, Mehlenbacher R, Sabatini R, McCamant DW (2009) Two-dimensional femtosecond stimulated Raman spectroscopy: Observation of cascading Raman signals in acetonitrile. *J Chem Phys* 131(21):214502.
13. Frostig H, Bayer T, Dudovich N, Eldar YC, Silberberg Y (2015) Single-beam spectrally controlled two-dimensional Raman spectroscopy. *Nat Photonics* 9(5):339–343.
14. Savolainen J, Ahmed S, Hamm P (2013) Two-dimensional Raman-terahertz spectroscopy of water. *Proc Natl Acad Sci USA* 110(51):20402–20407.
15. Hoffmann MC, Brandt NC, Hwang HY, Yeh KL, Nelson KA (2009) Terahertz Kerr effect. *Appl Phys Lett* 95(23):231105.
16. Allodi MA, Finneran IA, Blake GA (2015) Nonlinear terahertz coherent excitation of vibrational modes of liquids. *J Chem Phys* 143(23):234204.
17. Cho M (1999) Two-dimensional vibrational spectroscopy. III. Theoretical description of the coherent two-dimensional IR-Raman spectroscopy for the investigation of the coupling between both IR-and Raman-active vibrational modes. *J Chem Phys* 111(9):4140–4147.
18. Ikeda T, Ito H, Tanimura Y (2015) Analysis of 2D THz-Raman spectroscopy using a non-Markovian Brownian oscillator model with nonlinear system-bath interactions. *J Chem Phys* 142(21):212421.
19. Mukamel S (1999) *Principles of Nonlinear Optical Spectroscopy* (Oxford Univ Press, Oxford), Vol 6.
20. Hamm P, Savolainen J (2012) Two-dimensional-Raman-terahertz spectroscopy of water: Theory. *J Chem Phys* 136(9):094516.
21. Flanders B, Cheville R, Grischkowsky D, Scherer N (1996) Pulsed terahertz transmission spectroscopy of liquid $CHCl_3$, CCl_4, and their mixtures. *J Phys Chem* 100(29):11824–11835.
22. Shimanouchi T (1972) *Tables of Molecular Vibrational Frequencies Consolidated* (Natl Bureau Standards, Gaithersburg, MD), Vol I.
23. Huynh T, Anderson A (1997) Infrared and Raman study of solid dibromodichloromethane. *J Raman Spectrosc* 28(5):373–377.
24. Teo SM, Ofori-Okai BK, Werley CA, Nelson KA (2015) Invited Article: Single-shot THz detection techniques optimized for multidimensional THz spectroscopy. *Rev Sci Instrum* 86(5):051301.
25. Shalaby M, Hauri CP (2015) Demonstration of a low-frequency three-dimensional terahertz bullet with extreme brightness. *Nat Commun* 6:5976.
26. Tonouchi M (2007) Cutting-edge terahertz technology. *Nat Photonics* 1(2):97–105.
27. Hamm P, Zanni M (2011) *Concepts and Methods of 2D Infrared Spectroscopy* (Cambridge Univ Press, Cambridge, UK).
28. Leforestier C, et al. (1991) A comparison of different propagation schemes for the time dependent Schrödinger equation. *J Comput Phys* 94(1):59–80.